

1-1-2018

Estimation of the depth of anesthesia by using a multioutput least-square support vector regression

MERCEDEH JAHANSEIR

KAMAL SETAREHDAN

SIROUS MOMENZADEH

Follow this and additional works at: <https://journals.tubitak.gov.tr/elektrik>



Part of the [Computer Engineering Commons](#), [Computer Sciences Commons](#), and the [Electrical and Computer Engineering Commons](#)

Recommended Citation

JAHANSEIR, MERCEDEH; SETAREHDAN, KAMAL; and MOMENZADEH, SIROUS (2018) "Estimation of the depth of anesthesia by using a multioutput least-square support vector regression," *Turkish Journal of Electrical Engineering and Computer Sciences*: Vol. 26: No. 6, Article 2. <https://doi.org/10.3906/elk-1802-189>

Available at: <https://journals.tubitak.gov.tr/elektrik/vol26/iss6/2>

This Article is brought to you for free and open access by TÜBİTAK Academic Journals. It has been accepted for inclusion in Turkish Journal of Electrical Engineering and Computer Sciences by an authorized editor of TÜBİTAK Academic Journals. For more information, please contact academic.publications@tubitak.gov.tr.

Estimation of the depth of anesthesia by using a multioutput least-square support vector regression

Mercedeh JAHANSEIR¹ , Seyed Kamaledin SETAREHDAN^{2*} , Sirous MOMENZADEH³ 

¹Department of Biomedical Engineering, Science and Research Branch, Islamic Azad University, Tehran, Iran

²Control and Intelligent Processing Center of Excellence, School of Electrical and Computer Engineering, College of Engineering, University of Tehran, Tehran, Iran

³Functional Neurosurgery Research Center, Shahid Beheshti University of Medical Sciences, Tehran, Iran

Received: 25.02.2018

Accepted/Published Online: 08.06.2018

Final Version: 29.11.2018

Abstract: Today, most surgeries are performed under general anesthesia where one of the most growing methods for anesthesia depth monitoring is using electroencephalogram (EEG). The bispectral index (BIS) is the most commonly used parameter for anesthesia depth monitoring using EEG, the validity of which is still to be studied before being accepted as a routine method by clinicians. This paper proposes a new technique for detecting the depth of anesthesia by means of EEG, which is based on multioutput least-squares support vector regression (MLS-SVR), which provides the probability that the patient is in the four different possible anesthesia states. In this study, EEG signals were recorded from 20 patients who were anesthetized in the operation room. Twelve linear and nonlinear EEG features were then extracted every 10 s from the EEG signals to form the feature vector. The features were then classified by the MLS-SVR classifier and the results were compared with those of the BIS, where no significant differences were observed ($P > 0.05$). Due to using the MLS-SVR classifier, which replaces quadratic equations by linear equations, the proposed method shows a higher accuracy compared to the other previously reported methods.

Key words: Electroencephalogram, feature extraction, signal entropy, power spectral density, classification.

1. Introduction

Anesthesiologists recognize the depth of anesthesia in patients based on clinical observations (blood pressure, heart rate, respiration rate, eye tears, eye movement, sweating, and patient's physical response to stimulus). The inadequate use of anesthetic drugs causes consciousness during surgery. Light anesthesia has a catastrophic outcome on the patient, especially for those with a history of cardiac disease [1].

In order to prevent the above-mentioned incidents, using intelligent methods based on the body's physiological signals is considered an appropriate alternative. Therefore, in recent years, special attention has been paid to electroencephalogram (EEG) signal processing in order to estimate the depth of anesthesia [2, 3].

For awakening with closed eyes, EEG is active and typically shows prominent alpha activity (10 Hz). After administering a hypnotic drug, the patient enters a sedation state and EEG shows increased beta activity (13–25 Hz) [4]. After the sedation state, four stages occur: phase 1 is a light anesthetic state with decreased EEG beta activity (13–30 Hz) and increased alpha (8–12 Hz) and delta activities (0–4 Hz) [5, 6]. In phase 2, an intermediate state, beta activity decreases and alpha and delta activities increase [7]. During phase 3, a deeper state, EEG shows burst suppression. Surgery is often performed in phases 2 and 3. Phase 4 is the deepest

*Correspondence: ksetareh@ut.ac.ir

state, during which EEG is isoelectric [8]. Due to changes in the frequency bands of different states, it can be concluded that the power of frequency bands is an important feature in determining the depth of anesthesia, and considering these features is important for classification of anesthetic levels. Also, due to the nonlinear behavior of the brain, in addition to the frequency features, the entropy measure is also used to detect the depth of anesthesia. Frequency changes are measurable by the entropy criterion, and studies show progress in detecting the depth of anesthesia by different types of entropy [9, 10]. In [11], approximate entropy and permutation entropy were used as a features and SVMs were used to classify 2 states of anesthesia ('awake' and 'anesthetized' state). That study reported accuracy of 96 percent. Also, in [12], 2 states of anesthesia were classified with 95 percent accuracy. However, in the case of four-state anesthesia, [13] reported that the accuracy indices obtained by a modified SVM (GA-SVM) across the four patterns (relative power spectral density (PSD) of EEG band) were 90.64 ± 7.61 , 81.79 ± 5.84 , 82.14 ± 7.99 , and 72.86 ± 11.11 , respectively.

In this article, anesthesia was divided into five levels (awake, light to moderate sedation, superficial anesthesia, adequate anesthesia, and deep anesthesia) using the bispectral index (BIS) [14], a common criterion for determining the depth of anesthesia.

In this paper, the feature vector includes approximate entropy, permutation entropy, fractal dimension, detrended fluctuation analysis, Shannon entropy, and relative power of EEG bands and MLS-SVR classification was used to categorize anesthesia levels. Unlike the LS-SVR, this classifier is a multioutput classifier that expresses the possibility of the presence of each level of anesthesia. LS-SVR is a modified form of the SVR that solves linear equations and does not need to solve quadratic complex equations; thus, it reduces computational complexity and increases the calculation speed [15]. The capability of MLS-SVR is to be used online during anesthesia. Using the MLS-SVR classification, anesthetic levels were automatically determined with 88% accuracy.

2. Materials and methods

In this experimental study, features were extracted from every 10 s of an EEG signal recorded from 20 individuals during anesthesia. In calculating the features, the relative power of the frequency bands and the entropy measures were used. The final feature vector was classified using the MLS-SVR method. Finally, the results were evaluated for accuracy of classification. All steps are described in Sections 2 and 3 and the method's algorithm is shown in Figure 1.

2.1. Experimental dataset

In this research, the Saadat Co. Ltd. database was used. This dataset records monopolar Fpz-At1 from the forehead by BIS-QUATRO Sensor (Aspect Medical Systems, Newton, MA, USA). EEG signals of 20 individuals were recorded during anesthesia with a sampling rate of 200 Hz. In addition to raw EEG data, BIS and SQI (standard quality index) indices were also recorded. BIS was recorded at a frequency of 1.0 Hz. In this database, the age range of patients varied from 15 and 70 years[16].

2.2. Preprocessing

At first a notch filter was used to remove 50 HZ noise (Figure 2); in the second step, the *SQI* threshold was addressed. The quality of the signal was only validated when *SQI* > 80 and could be used in the signal analysis section.

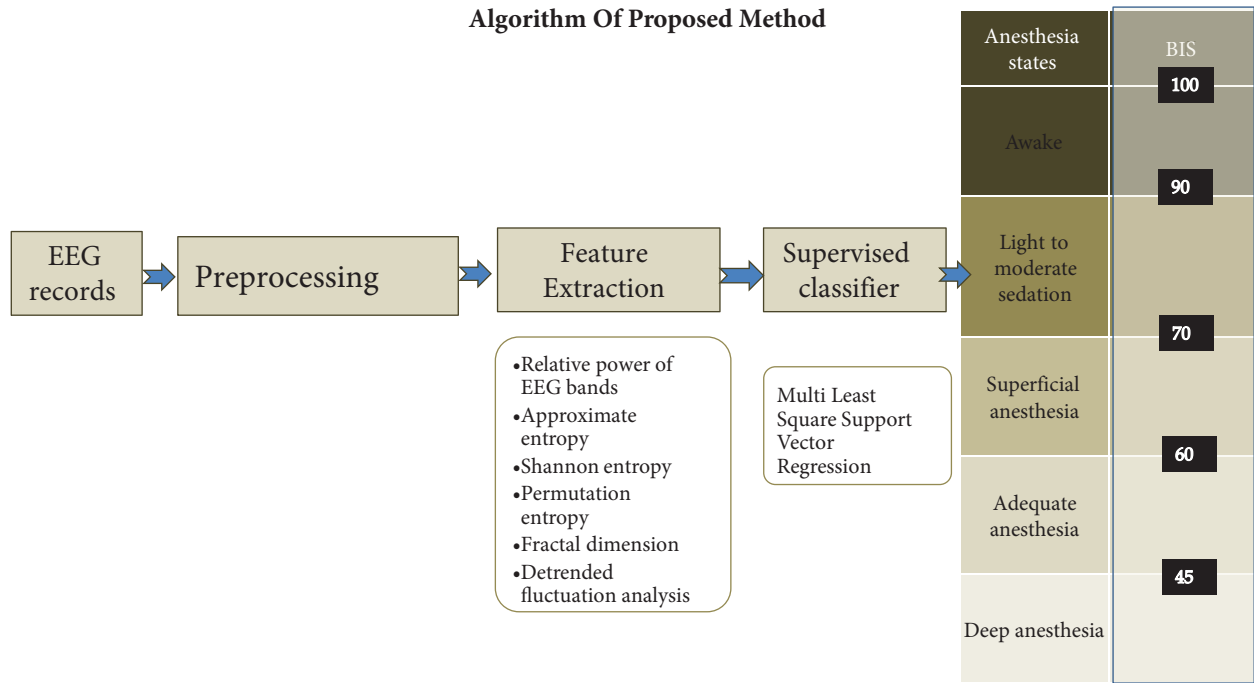


Figure 1. Features were extracted from the EEG signal and then the appropriate features were chosen. Finally, the classifier categorized the anesthesia states.

Different anesthetic levels are specified based on BIS in Table 1 [14]. Due to the limited valid data available in awake and light anesthesia phases, these two were considered as one state, and a total of 4 states were considered for anesthesia. An EEG signal recorded during anesthesia is shown in Figure 3a. Figure 3b shows the SQI corresponding to the EEG of Case 1.

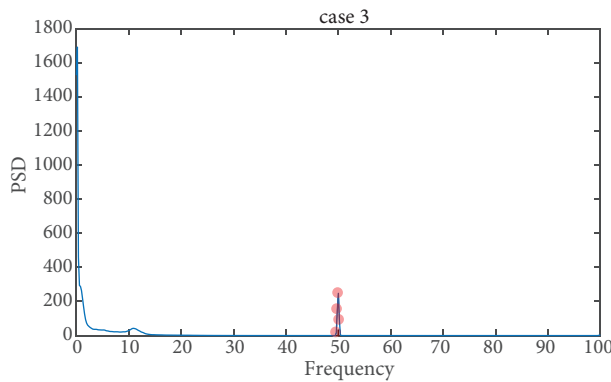


Figure 2. The PSD of the EEG signal; a notch filter was used to remove 50 HZ noise.

2.3. Feature extraction

Input data were a discrete time series to N length $x = \{x_1, \dots, x_N | x_i \in \mathbb{R}, i \in z > 0\}$ and the vector V , $V \in \mathbb{R}^q$, has q members, which shows the number of features. Features were extracted every 10 s from the signal. $v = \{v_1, \dots, v_q | v_j \in \mathbb{R}, j \in z > 0\}$. In the feature extraction step, the two approaches were considered. In the first approach, relative power spectral changes (delta (0–4 Hz), theta (4–7 Hz), alpha (8–12 Hz), low

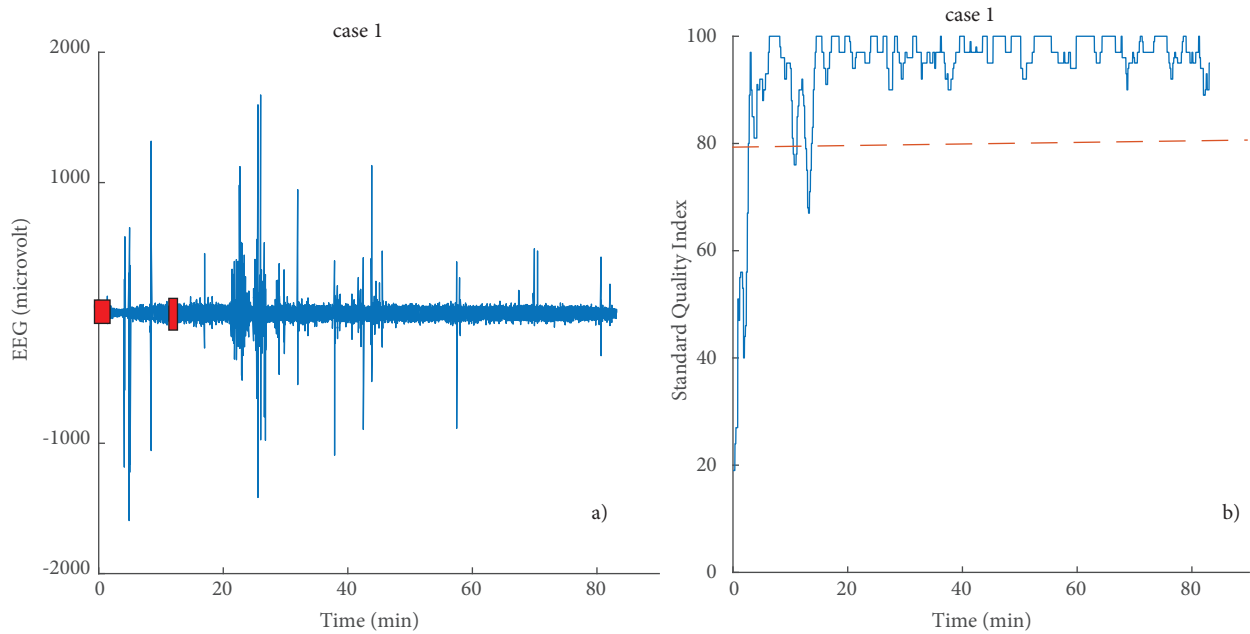


Figure 3. a. EEG signals were recorded during anesthesia and the quality of the signal was only accepted when $SQI > 80$; b. SQI corresponding to EEG signal in a.

Table 1. Anesthetic states based on BIS [14].

BIS	Anesthesia states
90 – 100	Awake
70 – 90	Light to moderate sedation
60 – 70	Superficial anesthesia
45 – 60	Adequate anesthesia
0 – 45	Deep anesthesia

beta (12–15 Hz), mid beta (15–18 Hz), high beta (22–35 Hz), gamma (35–70 Hz)) were evaluated at different levels of anesthesia, and in the second approach, due to regular EEG activity waves during anesthesia, features such as approximate entropy (ApEn), permutation entropy (PE), Shannon entropy (SE), detrended fluctuation analysis (DFA), and fractal dimension (FD) were investigated. In total, $q = 12$ features were extracted from EEG signals for complexity measures.

For computing the features, the standard algorithm was used [17]. Finally, all features were normalized based on $(x - \min(x))/(\max(x) - \min(x))$.

2.4. Classification (MLS-SVR)

This classifier is a modified type of LS-SVR with the difference that MLS-SVR learns the mapping from multiple inputs to multiple outputs. The standard LS-SVR algorithm is single-output, as briefly described below. If we consider inputs $x \in \mathbb{R}^d$ and outputs $y \in \mathbb{R}$, then $\{(x_i, y_i)\}_{i=1}^l$ is independent and identically distributed (i.i.d.); we consider $y = (y_1, y_1, \dots, y_1)^T \in \mathbb{R}^l$. The single-output LS-SVR solves the problem by finding two parameters, $\in \mathbb{R}^{n_h}$ & $b \in \mathbb{R}$, which minimizes the following cost function:

$$\min_{w \in \mathbb{R}^{n_h}, b \in \mathbb{R}} \mathcal{J}(w, \xi) = \frac{1}{2} w^T w + \gamma \frac{1}{2} \xi^T \xi, \tag{1}$$

$$s.t. \quad y = Z^T w + b \mathbf{1}_l + \xi. \tag{2}$$

$Z = (\varphi(x_1), \varphi(x_2), \dots, \varphi(x_l)) \in \mathbb{R}^{n_h \times l}$, $\varphi: \mathbb{R}^d \rightarrow \mathbb{R}^{n_h}$ is a vector consisting of Hilbert space with n_h dimension. $\xi = (\xi_1, \xi_2, \dots, \xi_l)^T \in \mathbb{R}^l$ is a vector consisting of slack variable and $\gamma \in \mathbb{R}_+$ is a positive real parameter. The single-output regression can simply be converted to m output, if we consider $Y = [i, j] \in \mathbb{R}^{l \times m}$. The samples are $\{(x_i, y^i)\}_{i=1}^l$ and $x_i \in \mathbb{R}^d$ and $y^i \in \mathbb{R}^m$. The purpose of multioutput regression is to predict $y \in \mathbb{R}^m$ from $x \in \mathbb{R}^d$ inputs. MLS-SVR solves the problem by finding two parameters if $w = (w_1, w_2, \dots, w_m) \in \mathbb{R}^{n_h \times m}$ and $b = (b_1, b_2, \dots, b_m)^T \in \mathbb{R}^m$, which minimizes the following cost function:

$$\min_{w \in \mathbb{R}^{m \times n_h}, b \in \mathbb{R}} \mathcal{J}(W, \Theta) = \frac{1}{2} \text{trace}(W^T W) + \gamma \frac{1}{2} \text{trace}(\Theta^T \Theta), \tag{3}$$

$$s.t. \quad Y = Z^T W + \text{repmat}(b^T, l, 1) + \Theta, \tag{4}$$

where $\Theta = (\xi_1, \xi_2, \dots, \xi_m) \in \mathbb{R}_+^{l \times m}$. $\text{repmat}(x, m, n)$ creates a matrix consisting of an $m \times n$ tiling of copies of x . For considering hierarchical Bayes insights, we assume that all $w_i \in \mathbb{R}^{n_h}$ ($i \in N_m$) can be written as $w_i = w_0 + v_i$. When the outputs are similar, the value of $v_i \in \mathbb{R}^{n_h}$ ($i \in N_m$) is low. Otherwise, the average $w_0 \in \mathbb{R}^{n_h}$ vector will be low. W_0 shows information about commonality and v_i ($i \in N_m$) shows information related to specialty. By finding two parameters of $w_0 \in \mathbb{R}^{n_h}$, $V = (v_1, v_2, \dots, v_m) \in \mathbb{R}^{n_h \times m}$ and $b = (b_1, b_2, \dots, b_m)^T \in \mathbb{R}^m$ the problem is solved, which minimizes the following cost function:

$$\min_{w_0 \in \mathbb{R}^{n_h}, V \in \mathbb{R}^{n_h}, b \in \mathbb{R}^m} \mathcal{J}(w_0, V, \Theta) = \frac{1}{2} w_0^T w_0 + \frac{1}{2} \gamma \text{trace}(V^T V) + \gamma \frac{1}{2} \text{trace}(\Theta^T \Theta), \tag{5}$$

$$s.t. \quad Y = Z^T W + \text{repmat}(b^T, l, 1) + \Theta, \tag{6}$$

where $\Theta = (\xi_1, \xi_2, \dots, \xi_m) \in \mathbb{R}_+^{l \times m}$, $W = (w_0 + v_1, w_0 + v_2, \dots, w_0 + v_m) \in \mathbb{R}^{n_h \times m}$, $Z = (\varphi(x_1), \varphi(x_2), \dots, \varphi(x_l)) \in \mathbb{R}^{n_h \times l}$, and $\gamma \in \mathbb{R}_+$ are two positive real parameters [15].

3. Results and discussion

For data analysis, MATLAB 2016b software was used on a macOS Sierra personal computer. The EEG signal was recorded from patients anesthetized in the operating theater, identified as case num. 1, case num. 2, ..., case num. 20.

Figure 4a shows an EEG spectrogram in the operating room. In this figure, reduced high frequency EEG bands during anesthesia with increased amplitude are shown during consciousness. The reason for this is the reduction of high frequency EEG band activity during anesthesia [3]. The frequency of EEG signal fluctuations is proportional to the level of consciousness and the level of the individual's concentration and their psychological/mental status in different frequency ranges [18]. The high power observed at 50 Hz is due to the city's electric noise. Figure 4b shows gamma band activity during anesthesia; initially the power of the gamma band is high, but the power reduces at the onset of anesthesia, and at the end of the operation, when the effect of an anesthetic drug is reduced, it indicates increased power. Anesthetic drugs reduce the activity

of the high frequency band, affecting the nervous system [19]. Reference [20] also reported reduced amplitude at high frequencies during deep anesthesia. Figure 4c shows increased beta band power during anesthesia. At the sedation stage, the strong activity of the beta band is seen at 15–30 Hz [21], and with the onset of deep anesthesia, the increased power of the β peak is transmitted to α [22]. As can be seen in Figure 4d, the power of the alpha band increases as the anesthesia starts. The reason for this is the regular activity of brain signals in anesthesia, which shows the power of alpha and delta frequency bands during anesthesia [4].

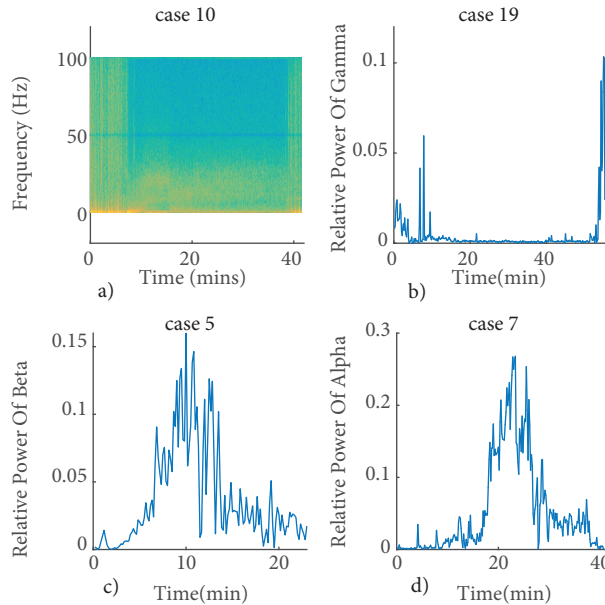


Figure 4. Brain signal spectrogram and variation of EEG band power during anesthesia.

In this paper, the feature vector, in addition to the relative power of EEG bands, included the entropy criterion. Features such as PE, APE, FD, and DFA showed regularity and irregularity in the brain signals and measure the complexity of the brain signals [17]. Table 2 shows the mean value of some of the features at different levels of consciousness. Features of this table did not show significant difference in t-tests with the BIS ($P > 0.05$). The trend of changes in features such as PE, gamma, beta, and theta bands are proportional to the depth of anesthesia in terms of BIS. The magnitude of these features increases or decreases with increased depth of anesthesia.

Table 2. Average normalized values of features at various anesthetic levels.

States	Features						
	APEN	SE	Relative POWER alpha	Relative POWER theta	Relative POWER high beta	Relative POWER gamma	PE
Awake & light to moderate sedation	0.0749	0.057	0.027	0.016	0.0285	0.00481	0.856
Superficial anesthesia	0.0295	0.0370	0.0691	0.0277	0.0194	0.002216	0.872
Adequate anesthesia	0.0279	0.0107	0.0854	0.0417	0.00554	0.00090	0.819
Deep anesthesia	0.03861	0.0360	0.07663	0.04318	0.0029	0.0005	0.721

Figure 5a shows the trend of changes in PE and BIS index. The PE criterion specifies the signal complexity by determining the irregularity level in the signal. Typically, for a single-frequency periodic signal, PE is near zero, while it is large for a random signal [23]. Reference [24] also used the PE feature to detect the depth of anesthesia. Figure 5b shows the trend of FD changes and BIS index. Reference [25] also described FD as a useful feature for detecting the depth of anesthesia.

Table 3 shows the confusion matrix for classifying all data. Due to limited data from the awake phase, the data of awake and light anesthesia phases were grouped into one group. The accuracy of the MLS-SVM classifier was 88%.

At the end of classification, accuracy results that are TP Rate, FP Rate, Precision, Recall, and ROC area values for MLS-SVR are given in Table 4.

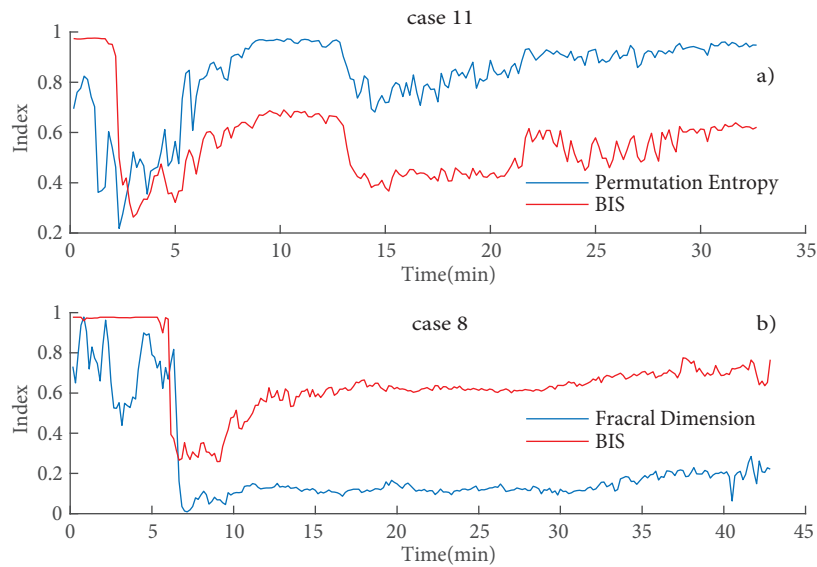


Figure 5. a. Changes in BIS and PE indices (case num. 11). b. Changes in BIS and FD indices (case num. 9).

Table 3. Confusion matrix of MLS-SVR classifier.

		Predicted value			
		Awake & light to moderate sedation	Superficial anesthesia	Adequate anesthesia	Deep anesthesia
Actual Value	Awake & light to moderate sedation	205	30	3	2
	Superficial anesthesia	26	515	15	3
	Adequate anesthesia	22	20	370	38
	Deep anesthesia	10	1	33	395

4. Conclusion

In this study, EEG signals were analyzed and evaluated to extract the features and compare them with the BIS for detecting the depth of anesthesia. The features of EEG frequency bands and the types of entropy

Table 4. Prediction results for classification method.

Multioutput least-square support vector regression					
	TP Rate	NP Rate	Precision	Recall	ROC Area
C1	0.854	0.04	77.947%	85.417%	0.90
C2	0.9213	0.0443	90.989%	92.129%	0.93
C3	0.8222	0.0401	87.886%	82.222%	0.89
C4	0.8998	0.0346	90.183%	89.977%	0.93
Avg	0.8758	0.3975	87%	87.43%	0.91
Overall accuracy = 88%		Kappa = 0.836			

(relative power of EEG band and entropy measures) used in this article had no significant difference with the BIS criterion ($P > 0.05$). In this article nonlinear features such as PE, FD, APE, SE, DFA, and linear features in the frequency domain were used. The nonlinear features could successfully track changes in the consciousness and alertness of the subjects in the operating room [26]. Moreover, since the EEG activity during anesthesia were regularized, and the spectral density of EEG bands can show the difference between anesthesia states [27].

Many different techniques like ANN and SVR were used for EEG signal classification in the past [28]. For nonlinear multiclass classification, SVR and SVM are mostly used since they build an optimized hyperplane. SVR and SVM based regression techniques solve some ANN problems like the nonuniqueness of the final ANN solution [29].

In comparison with different types of classifiers, in this article the main attention is drawn to the use of SVR. LS-SVR is a modified form of SVR where the difference is that LS-SVR solves a set of linear equations, instead of solving the quadratic programming problem, and causes low computational complexity so it reduces the imposed costs and increases the speed and accuracy. MLS-SVR is a modified form of LS-SVR but has multiple outputs instead of one.

Using the MLS-SVR classifier, the anesthetic levels were automatically classified. The reason for choosing this classifier was it being multioutput and its ability to run online. It can also use the data instantaneously imported to the machine in order to update. For anesthesiologists, a classifier model that can analyze EEG signals and conduct classification process automatically in a short time with high accuracy is necessary [30].

The advantages of the proposed features compared to the BIS include a clear implementation algorithm and the physiologic justification of these features (the regular activity of brain neurons during anesthesia).

Finally, optimization of the processing methods used in order to increase their speed and accuracy and studying other EEG-derived variables able to estimate the depth of anesthesia are recommended.

References

- [1] Miller RD, Pardo M. Basics of Anesthesia. 6th ed. Philadelphia, PA, USA: Elsevier Saunders, 2011.
- [2] Wang J, Zhang L, Huang Q, Wu G, Weng X, Lai Z, Lin P. Monitoring the end-tidal concentration of sevourane for preventing awareness during anesthesia (MEETS-PANDA): a prospective clinical trial. *Int J Surg* 2017; 41: 44-49.
- [3] Li D, Hambrecht-Wiedbusch VS, Mashour GA. Accelerated recovery of consciousness after general anesthesia is associated with increased functional brain connectivity in the high-gamma bandwidth. *Front Syst Neurosci* 2017; 11: 16.

- [4] Gaskell AL, Hight DF, Winders J, Tran G, Defresne A, Bonhomme V, Raz A, Sleigh JW, Sanders RD. Frontal alpha-delta EEG does not preclude volitional response during anaesthesia: prospective cohort study of the isolated forearm technique. *Br J Anaesth* 2017; 119: 664-673.
- [5] Vasella FC, Frascarolo P, Spahn DR, Magnusson L. Antagonism of neuromuscular blockade but not muscle relaxation affects depth of anaesthesia. *Br J Anaesth* 2005; 94: 742-747.
- [6] Guignard B. Monitoring analgesia. *Best Pract Res Clin Anaesthesiol* 2006; 20: 161-180.
- [7] Chernik DA, Gillings D, Laine H, Hendler J, Silver JM, Davidson AB, Schwam EM, Siegel JL. Validity and reliability of the Observer's Assessment of Alertness/Sedation Scale: study with intravenous midazolam. *J Clin Psychopharmacol* 1990; 10: 244-251.
- [8] Lan JY, Abbod MF, Yeh RG, Fan SZ, Shieh JS. Intelligent modeling and control in anesthesia. *J Med Biol Eng* 2012; 32: 293-308.
- [9] Liu Q, Wei Q, Fan SZ, Lu CW, Lin TY, Abbod MF, Shieh JS. Adaptive computation of multiscale entropy and its application in EEG signals for monitoring depth of anesthesia during surgery. *Entropy* 2012; 14: 978-992.
- [10] Mueller JN, Kreuzer M, Garcia PS, Schneider G, Hautmann H. Monitoring depth of sedation: evaluating the agreement between the Bispectral Index, qCON and the Entropy Module's State Entropy during exible bronchoscopy. *Minerva Anesthesiol* 2017; 83: 563-573.
- [11] Nicolaou N, Houris S, Alexandrou P, Georgiou J. Entropy measures for discrimination of awake vs anaesthetized state in recovery from general anesthesia. In: *IEEE 2011 Engineering in Medicine and Biology Society Annual International Conference*; 30 August–3 September 2011; Boston, MA, USA. New York, NY, USA: IEEE. pp. 2598-2601.
- [12] Nicolaou N, Houris S, Alexandrou P, Georgiou J. Permutation entropy for discriminating conscious and unconscious state in general anesthesia. In: *Engineering Applications of Neural Networks conference*; 2011. Berlin, Germany: Springer. pp. 280-288.
- [13] Liang Z, Huang C, Li Y, Hight DF, Voss LJ, Sleigh JW, Li X, Bai Y. Emergence EEG pattern classification in sevoflurane anesthesia. *Physiol Meas* 2018; 39: 045006.
- [14] Nunes RR, Chave IM, Alencar JC, Franco SB, Oliveira YG, Menezes DG. Bispectral index and other processed parameters of electroencephalogram: an update. *Rev Bras Anesthesiol* 2012; 62: 111-117.
- [15] Xu S, An X, Qiao X, Zhu L, Li L. Multi-output least-squares support vector regression machines. *Pattern Recognit* 2013; 34: 1078-1084.
- [16] Shalhaf R, Behnam H, Moghadam HJ, Mehrnam A, Sadaghiani M. The brain function index as a depth of anesthesia indicator using complexity measures. In: *IEEE 2013 Systems, Process and Control Conference*; 13–15 December 2013; Kuala Lumpur, Malaysia. New York, NY, USA: IEEE. pp. 68-72.
- [17] Rodriguez-Sotelo JL, Osorio-Forero A, Jimnez-Rodrguez A, Cuesta-Frau D, Cirugeda-Roldn E, Peluffo D. Automatic sleep stages classification using EEG entropy features and unsupervised pattern analysis techniques. *Entropy* 2014; 16: 6573-6589.
- [18] Caviness JN, Lue LF, Hentz JG, Schmitz CT, Adler CH, Shill HA, Sabbagh MN, Beach TG, Walker DG. Cortical phosphorylated Synuclein levels correlate with brain wave spectra in Parkinson's disease. *Mov Disord* 2016; 31: 1012-1019.
- [19] Reed S. Differential effects of propofol on gamma-band activity across cortical and thalamic sites in the rat, in vivo. PhD, McGill University, Montreal, Canada, 2012.
- [20] Breshears JD, Roland JL, Sharma M, Gaona CM, Freudenburg ZV, Tempelhoff R, Avidan MS, Leuthardt EC. Stable and dynamic cortical electrophysiology of induction and emergence with propofol anesthesia. *P Natl Acad Sci USA* 2010; 107: 21170-21175.
- [21] Dumont GA. Monitoring the EEG for assessing depth of anesthesia. In: *Monitoring Technologies in Acute Care Environments conference*; 2014. New York, NY, USA: Springer. pp. 255-260.

- [22] Hashemi M, Hutt A, Hight D, Sleigh J. Anesthetic action on the transmission delay between cortex and thalamus explains the beta-buzz observed under propofol anesthesia. *PLoS One* 2017; 12: e0179286.
- [23] Zunino L, Olivares F, Scholkmann F, Rosso OA. Permutation entropy based time series analysis: equalities in the input signal can lead to false conclusions. *Phys Lett A* 2017; 381: 1883-1892.
- [24] Su C, Liang Z, Li X, Li D, Li Y, Ursino M. A comparison of multiscale permutation entropy measures in on-line depth of anesthesia monitoring. *PLoS One* 2016; 11: e0164104.
- [25] Kuhlmann L, Manton JH, Heyse B, Vereecke HE, Lipping T, Struys M, Liley DT. Tracking electroencephalographic changes using distributions of linear models: application to propofol-based depth of anesthesia monitoring. *IEEE T Biomed Eng* 2017; 64: 870-881.
- [26] Widman G, Schreiber T, Rehberg B, Hoefft A, Elger CE. Quantification of depth of anesthesia by nonlinear time series analysis of brain electrical activity. *Phys Rev E* 2000; 62: 4898-4903.
- [27] Nguyen-Ky T, Wen P, Li Y, Gray R. Measuring and reflecting depth of anesthesia using wavelet and power spectral density. *IEEE T Inf Technol B* 2011; 15: 630-639.
- [28] Aditya S, Tibarewala DN. Comparing ANN, LDA, QDA, KNN and SVM algorithms in classifying relaxed and stressful mental state from two-channel prefrontal EEG data. *International Journal of Artificial Intelligence and Soft Computing* 2012; 3: 143-164.
- [29] Majumdar K. Human scalp EEG processing: various soft computing approaches. *Appl Soft Comput* 2011; 11: 4433-4447.
- [30] Deng C, Xu J, Zhang K, Tao D, Gao X, Li X. Similarity constraints-based structured output regression machine: An approach to image super-resolution. *IEEE T Neural Netw Learn Syst* 2016; 27: 2472-2485.